Electronic Supplementary Material (ESI) for New Journal of Chemistry.

Supplementary Information (SI)

Asymmetrical Zr_2CO/VSe_2 Heterostructure as Efficient Electrocatalysts for Hydrogen Evolution Reaction

Jisong Hu,[a] Xiangyu Liu,[b] Jiahao Wang,[b] Jinxuan Jin,[b] Ming Ouyang,[b] Moshang Fan,[a] Rui Zhang,[c] Xiao Ji[a], Ling Miao*[a] and Jianjun Jiang[a]

[a] *School of Optical and Electronic Information, Huazhong University of Science and Technology, Luoyu Road 1037, Wuhan, 430074, PR China. E-mail: miaoling@hust.edu.cn*

[b] *School of Integrated Circuits, Huazhong University of Science and Technology, Luoyu Road 1037, Wuhan, 430074, PR China*

[c] *School of Chemical and Environmental Engineering, Shanghai Institute of Technology, Shanghai, 201418, PR China*

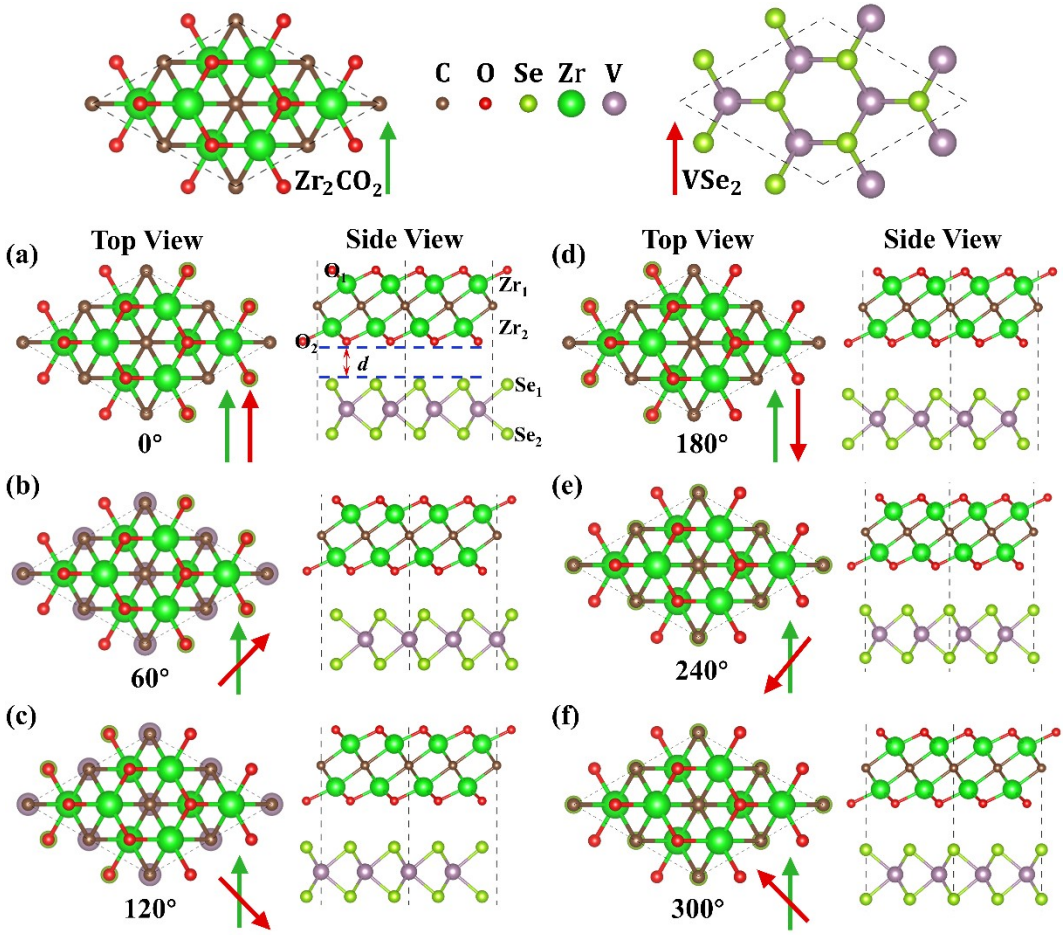

Fig. S1 Schematic representations of symmetric Zr_2CO_2/VSe_2 heterostructure, illustrating the correlation between different patterns and their respective stacking angles: (a) 0° for T1, (b) 60° for T2, (c) 120° for T3, (d) 180° for T4, (e) 240° for T5, and (f) 300° for T6.

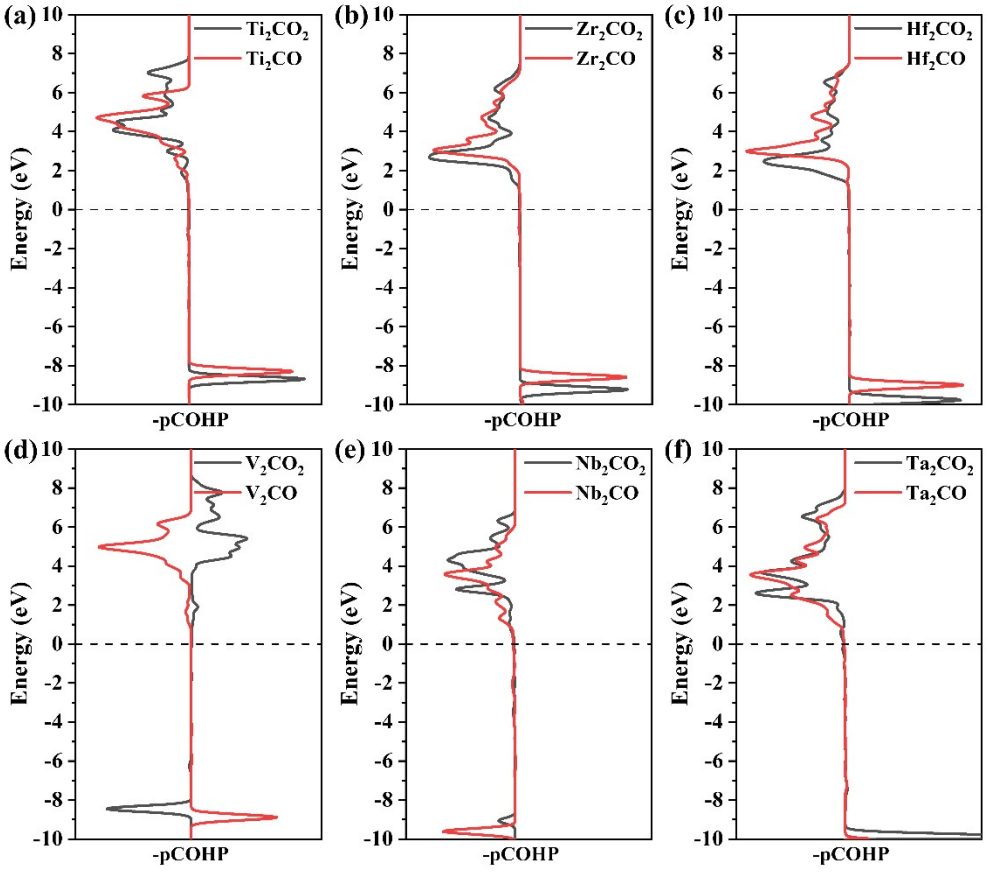

Fig. S2 Calculated partial crystal orbital hamilton population (pCOHP) for H−O bonds in hydrogen-adsorbed structures: (a) Ti_2CO_2 vs. Ti_2CO, (b) Zr_2CO_2 vs. Zr_2CO, (c) Hf_2CO_2 vs. Hf_2CO, (d) V_2CO_2 vs. V_2CO, (e) Nb_2CO_2 vs. Nb_2CO, (f) Ta_2CO_2 vs. Ta_2CO.

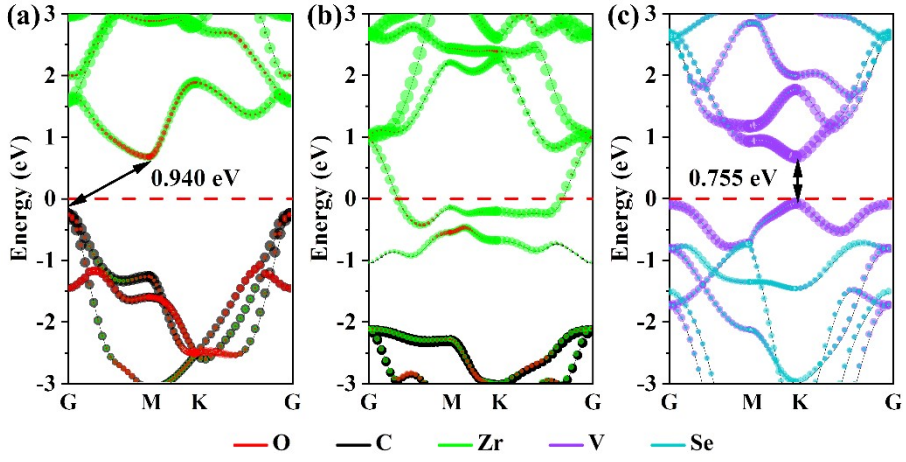

Fig. S3 Band structure diagrams of (a) Zr_2CO_2, (b) Zr_2CO, and (c) VSe_2.

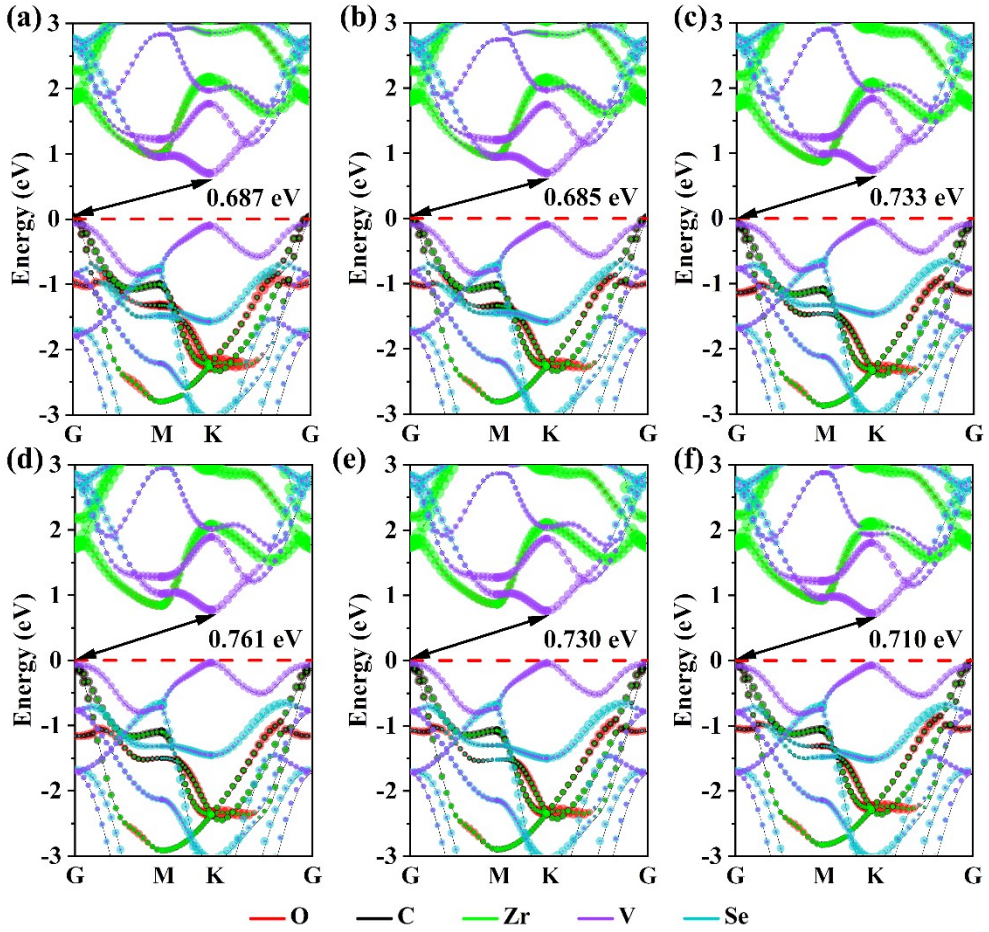

Fig. S4 Band structure diagrams for the Zr_2CO_2/VSe_2 heterostructure in various configurations: (a) T1, (b) T2, (c) T3, (d) T4, (e) T5, and (f) T6.

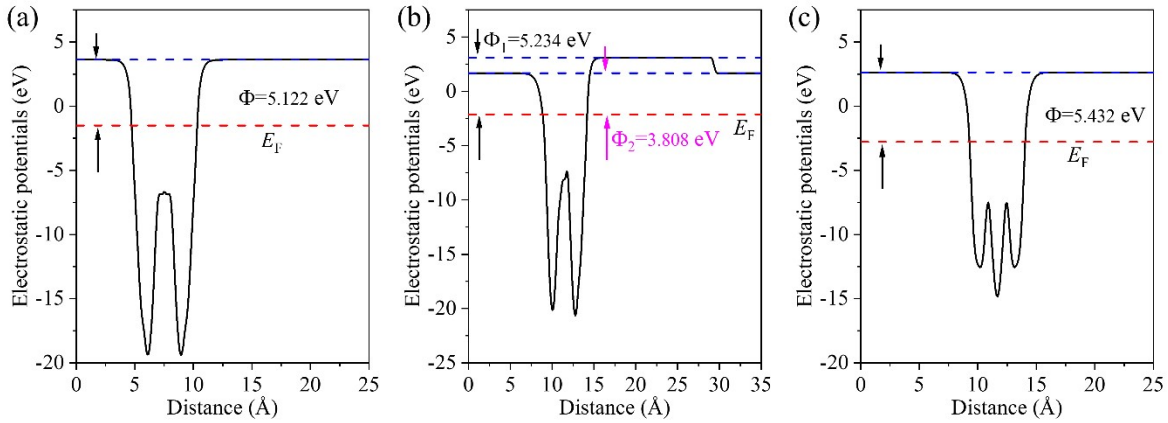

Fig. S5 Work function diagrams for Zr_2CO_2, Zr_2CO, and VSe_2.

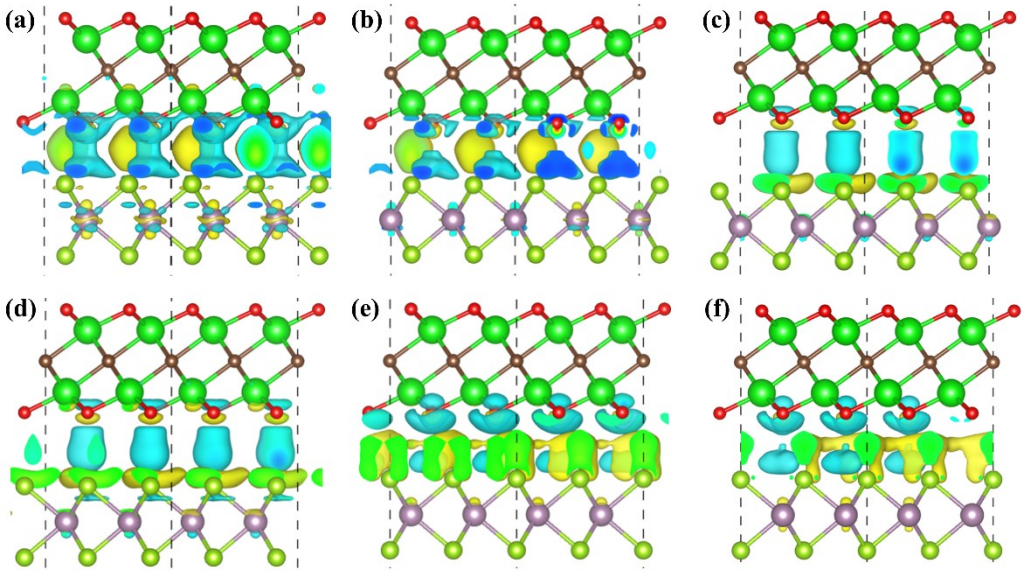

Fig. S6 Three-dimensional charge density difference for the Zr_2CO_2/VSe_2 heterostructure in various configurations: (a) T1, (b) T2, (c) T3, (d) T4, (e) T5, and (f) T6, illustrating charge accumulation (yellow) and depletion (cyan) with an iso-surface value of 0.0001 e/Å^3.

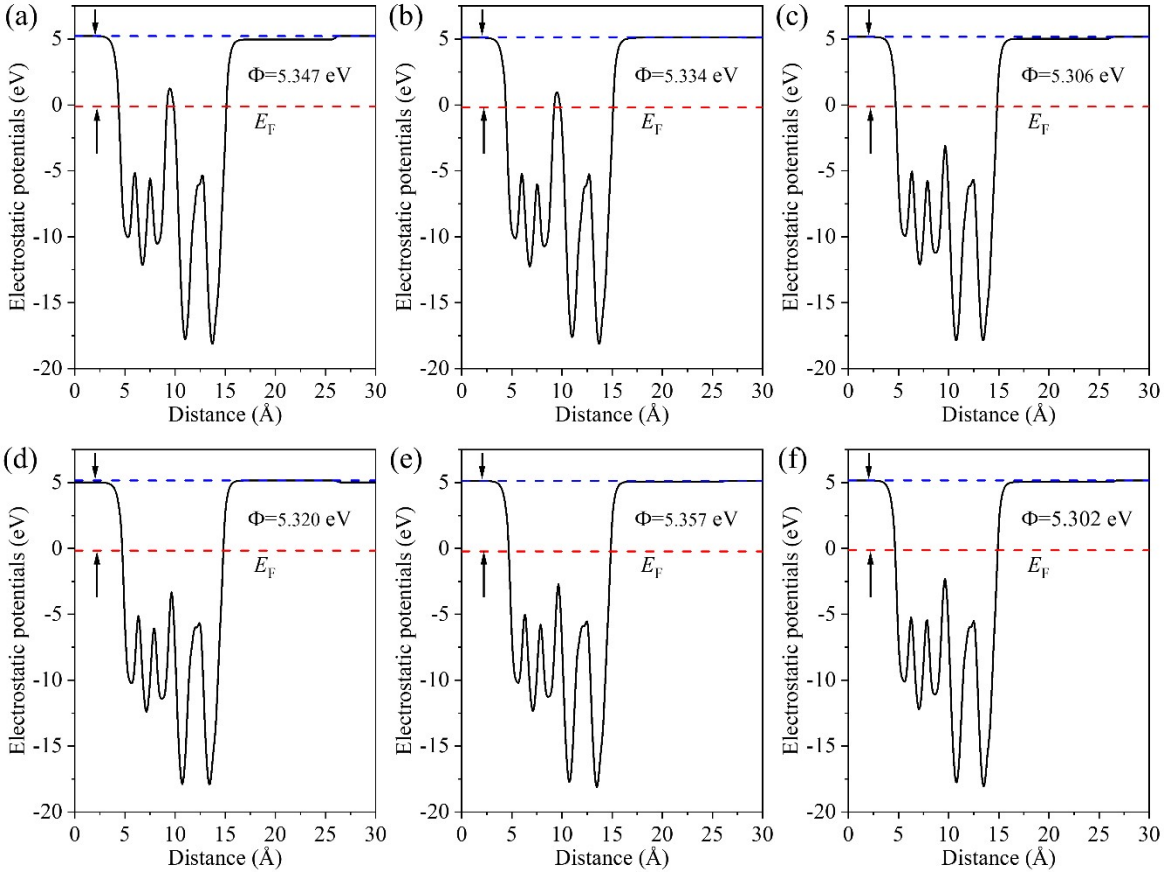

Fig. S7 Work functions of the Zr_2CO/VSe_2 heterostructure in various stacking configurations: (a) T1, (b) T2, (c) T3, (d) T4, (e) T5, and (f) T6.

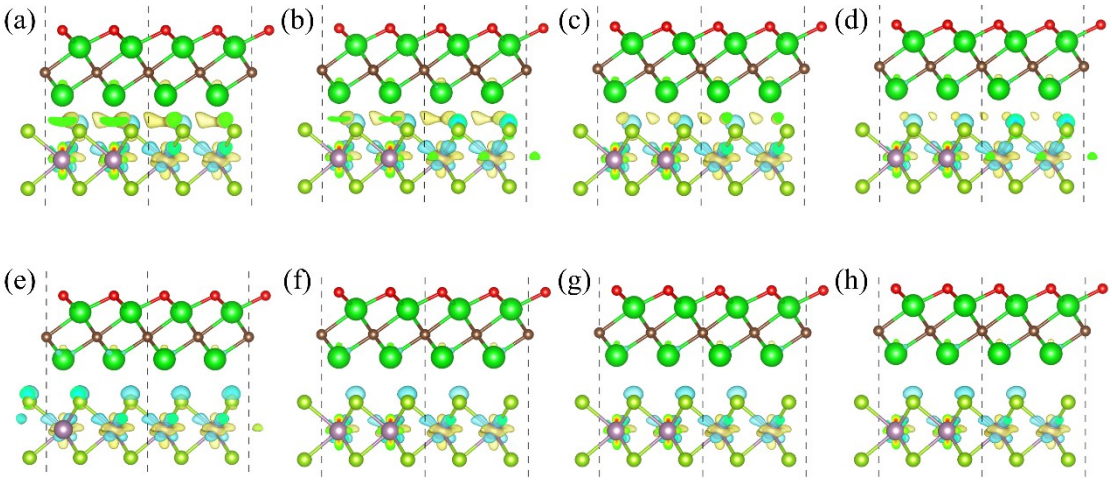

Fig. S8 Three-dimensional charge density differences for the T4 configuration of the Zr_2CO/VSe_2 heterostructure at various interlayer spacings: (a) 2.0 Å, (b) 2.1 Å, (c) 2.2 Å, (d) 2.3 Å, (e) 2.4 Å, (f) 2.5 Å, (g) 2.6 Å, (h) 2.7 Å. The charge accumulation/depletion is shown in yellow/cyan with an iso-surface of 0.005 e/Å^3.

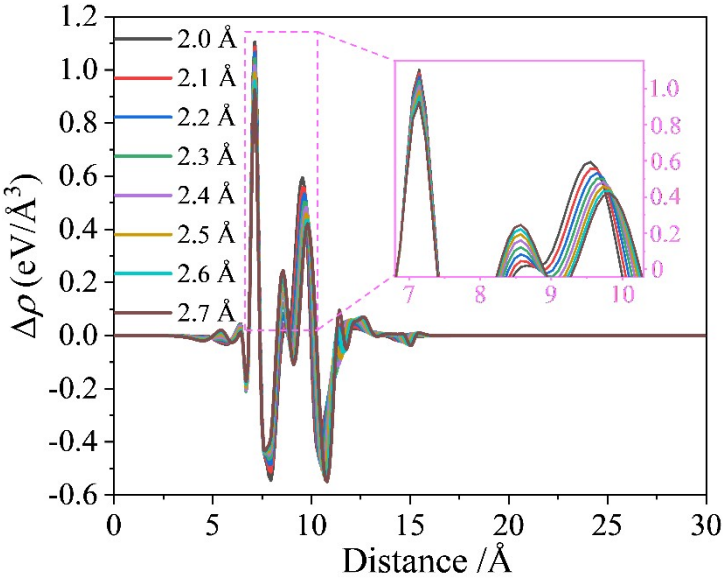

Fig. S9 Planar-averaged charge density difference for the T4 configuration at different interlayer spacings.

Table S1 Lattice constants of Zr_2CO_2, Zr_2CO and VSe_2

Structure	a /Å	b /Å	α /°	β /°	γ /°
Zr_2CO_2	3.290	3.290	90	90	120
Zr_2CO	3.263	3.263	90	90	120
VSe_2	3.319	3.319	90	90	120

Table S2 Lattice parameters, interlayer spacings, binding energies, and ΔG_{H^*} values for the Zr_2CO_2/VSe_2 heterostructure at various stacking angles

Structures	Rotation angle (°)	Lattice parameters (Å)	Layer spacing (Å)	Binding energy (meV/Å^2)	ΔG_{H^*} (eV)	
					O side	Se side
T1	0	6.589	2.810	−14.289	0.725	0.660
T2	60	6.596	2.844	−20.343	0.759	0.657
T3	120	6.605	3.002	−25.631	0.828	0.673
T4	180	6.580	3.336	−7.193	0.804	0.674
T5	240	6.581	2.966	−12.866	0.810	0.673
T6	300	6.604	3.005	−25.524	0.805	0.672

Table S3 Bader charges of the T4 configuration across varying interlayer spacings

Layer spacing /Å	Bader charges /e						
	O	Zr_1	C	Zr_2	Se_1	V	Se_2
2.0	7.263	9.804	5.982	10.375	7.066	11.945	6.564
2.1	7.264	9.809	5.992	10.400	7.029	11.941	6.565
2.2	7.265	9.812	5.998	10.392	7.034	11.934	6.566
2.3	7.262	9.815	5.999	10.421	7.008	11.929	6.567
2.4	7.260	9.816	6.000	10.441	6.991	11.923	6.568
2.5	7.255	9.812	6.012	10.467	6.967	11.918	6.569
2.6	7.256	9.800	6.025	10.490	6.946	11.912	6.571
2.7	7.260	9.802	6.018	10.518	6.925	11.904	6.574